Three-Dimensional Modeling of Conditioned and Unconditioned Basement Thermal Performance

William P. Bahnfleth, Ph.D., P.E.
Member ASHRAE

Cynthia A. Cogil
Associate Member ASHRAE

Grenville K. Yuill, Ph.D., P.E.
Fellow ASHRAE

ABSTRACT

A detailed, three-dimensional numerical model of the thermal performance of conditioned and unconditioned residential basements is described. The model has the ability to simulate a basement's geometry, construction, insulation treatment, and environmental control in detail. Hourly weather data are taken from standard Typical Meteorological Year (TMY) files. The transient foundation and soil temperature distributions are calculated using an ADI finite-difference numerical technique for a one-hour time step. A ground surface heat balance accounts for conduction, radiation, convection, and evapotranspiration. On the portion of the foundation wall extending above grade and along interior basement surfaces, both convective and radiative effects are modeled. Unconditioned basement air temperature is computed at each time step by a heat balance algorithm. Capabilities of the model are illustrated through representative case studies.

INTRODUCTION

The study of basement heat transfer is justified by the extent to which an uninsulated basement influences the total space conditioning energy consumption and peak loads of a typical house, by the large number of new homes being built with basements, and by the widespread use of basements as livable space. An uninsulated basement that accounted for 10% to 20% of the design heat loss of a typical home of the mid-1970s (Meixel et al. 1979) would now account for two to three times that percentage due to improved sealing and insulation above grade (Christian 1991; Labs et al. 1988; Shipp 1983; Wielhouwer 1982). The U.S. Bureau of the Census (1995) estimates that approximately 40% of all new single-family homes built in the United States and 85% of those in the Northeast have basements. Approximately 30% of basements constructed today are finished and considered habitable space (Christian 1988).

Prior investigations focused on the modeling of earth-coupled heat transfer have included multi-dimensional finite-difference (FDM) and finite-element (FEM) numerical methods and simplified methods developed from detailed modeling (Wang 1979; Shipp 1979; Szydlowski and Kuehn 1981; Richmond and Besant 1985; Bahnfleth 1989; Mitalas 1982; Krarti and Choi 1996). Nevertheless, the procedure of the American Society of Heating, Refrigerating and Air-Conditioning Engineers (ASHRAE) for predicting basement design heat loss using steady-state analysis (ASHRAE 1997; Latta and Boileau 1969) remains in common use although the assumptions underlying this procedure lack validity for heavily insulated foundation walls and partial insulation.

Research into the modeling of earth-coupled heat transfer over the last few decades has yielded many useful insights; however, advancements produced by one study have not necessarily been incorporated in the next study and there exists no consensus model of basement heat transfer. Published models differ in details of foundation type and insulation configuration, boundary conditions, treatment of three-dimensional effects, interior and exterior ambient conditions, and other important aspects. All of these factors influence the ground temperature distribution and foundation heat loss. Given the lack of consensus regarding appropriate methodology and the prevalence of sweeping assumptions in the analysis of earth-coupled heat transfer, a further investigation using detailed models is justified.

This paper describes a recently developed, detailed three-dimensional numerical model of basement heat transfer. The model is intended for use as a research tool in the study of load and energy estimation procedures and in the evaluation of the performance of a variety of basement insulation configura-

William P. Bahnfleth is an assistant professor of architectural engineering at Penn State University, University Park, Penn. **Cynthia A. Cogil** is an engineer-in-training at KCF-SHG, Washington, D.C. **Grenville K. Yuill** is director of Architectural Engineering at the University of Nebraska, Omaha.

tions. At present, the model runs in stand-alone mode, and interactions with the above-ground structure are handled in a simplified manner. However, work in progress will integrate the model with a whole-building energy analysis program. Similarly, certain important effects such as infiltration and internal heat gains from space conditioning equipment, appliances, and lighting are not presently included in the model but will be added as its development continues. Discussion of model features and modeling techniques is followed by illustrative examples of its capabilities.

Three-dimensional effects in basement heat transfer have been shown to be important by both Mitalas (1987) and Walton (1987). Walton's comparisons of two- and three-dimensional basement heat transfer models indicated that errors could be as large as 50%. Mitalas attempted to account for three-dimensional effects by means of corner correction factors. Walton proposed an efficient quasi-three-dimensional numerical technique that agreed closely with full three-dimensional modeling for the test cases he considered. The recognized importance of three-dimensional effects justifies the development and maintenance of fully three-dimensional models for fundamental research and as a check on approximate methods. Further, heat transfer is not the only three-dimensional effect of interest. The effect of cold corners on the formation of condensation, thermal bridging, structural analysis of foundations under freezing soil conditions, and thermal comfort studies are examples of practical concerns that require or would benefit from the use of a three-dimensional heat transfer model.

MODEL DEVELOPMENT

With several significant improvements and enhancements, the present basement model is based on the slab-on-grade model developed previously by Bahnfleth (1989). This section surveys model features and methodology. Cogil (1998) provides a more detailed discussion of these topics.

MODEL FEATURES

Both conditioned and unconditioned basements can be simulated. Heat transfer components modeled include the below-ground foundation wall and basement floor, above-ground foundation wall, and basement ceiling. Infiltration and internal loads have not been incorporated in the model, but it would be straightforward to do so. Future development of the model will address these effects.

In addition to conventional cast-in-place concrete foundations, the model can simulate a pressure-treated wood, cast-in-place concrete with insulating concrete forms, and precast insulated concrete panels. For cast-in-place concrete, three common (Christian 1991; Labs et al. 1988) insulation configurations are modeled: full-height exterior; full-height interior; and partial-height exterior covering the upper half of the foundation wall, as shown in Figures 1a through 1c. For unconditioned basements, insulation between floor joists can be modeled, as shown in Figure 1d. Insulation is modeled as having negligible thermal mass, enabling it to be treated as a pure thermal resistance added to either side of the foundation wall. This eliminates the need to redefine the grid. When insulation is one component in an assembly of materials, such as a wood frame wall, the average overall R-value of the insulation assembly is calculated assuming parallel heat flow paths.

When uninsulated, the sill box (the portion of the foundation wall composed of the sill plate and rim joist) is a significant heat flow path due to the limited thermal resistance of exterior sheathing and siding. In cases with exterior insulation, it is assumed that foundation insulation extended above grade beneath an overhanging frame to insulate the sill box. Similarly, the same R-value of insulation applied to the interior surface of the foundation wall is applied to the interior surface of the rim joist.

The air temperature in an unconditioned basement is determined by a quasi-steady heat balance that includes both convection and radiant surface exchanges. Most previous analyses of conditioned basements have assumed that the basement air temperature is maintained at a constant seasonal setpoint temperature and that all nonzero heat transfer can be identified as either a heating or cooling load on space conditioning equipment. In reality, there are periods of significant duration during which acceptable indoor conditions are maintained without operation of heating or cooling equipment by allowing indoor conditions to float or through occupant intervention, for example, by opening windows for cooling during moderately warm weather. The range of conditions for which this mode of operation occurs is referred to herein as the "dead-band." Detailed modeling of this interaction would require the coupling of the basement model with a whole building model, which will take place in a future stage of development. For the present, dead-band operation and its effects have been modeled in a simplified manner, which, nevertheless, is considerably more realistic than environmental control assumptions of previous models.

As a first approximation, conditions under which dead-band operation occurs can be aliased to outdoor dry-bulb temperatures determined through analysis of the energy consumption history of a house. The boundaries of the dead-band are essentially the heating and cooling balance point temperatures. For the purposes of this model, the above-ground conditioned space temperature is assumed to equal the seasonal setpoint when outdoor dry-bulb temperature falls outside the dead-band and is determined by interpolation when outdoor dry bulb is within the dead-band. As in the case of an unconditioned basement, the air temperature in a conditioned basement is variable during dead-band operation and must be computed by means of an energy balance.The assumption of a dead-band in which no mechanical space conditioning occurs makes it possible to estimate equipment heating and cooling loads due to the basement, as distinct from net positive and negative heat transfers. In the case of a conditioned basement, annual heating and cooling loads are the

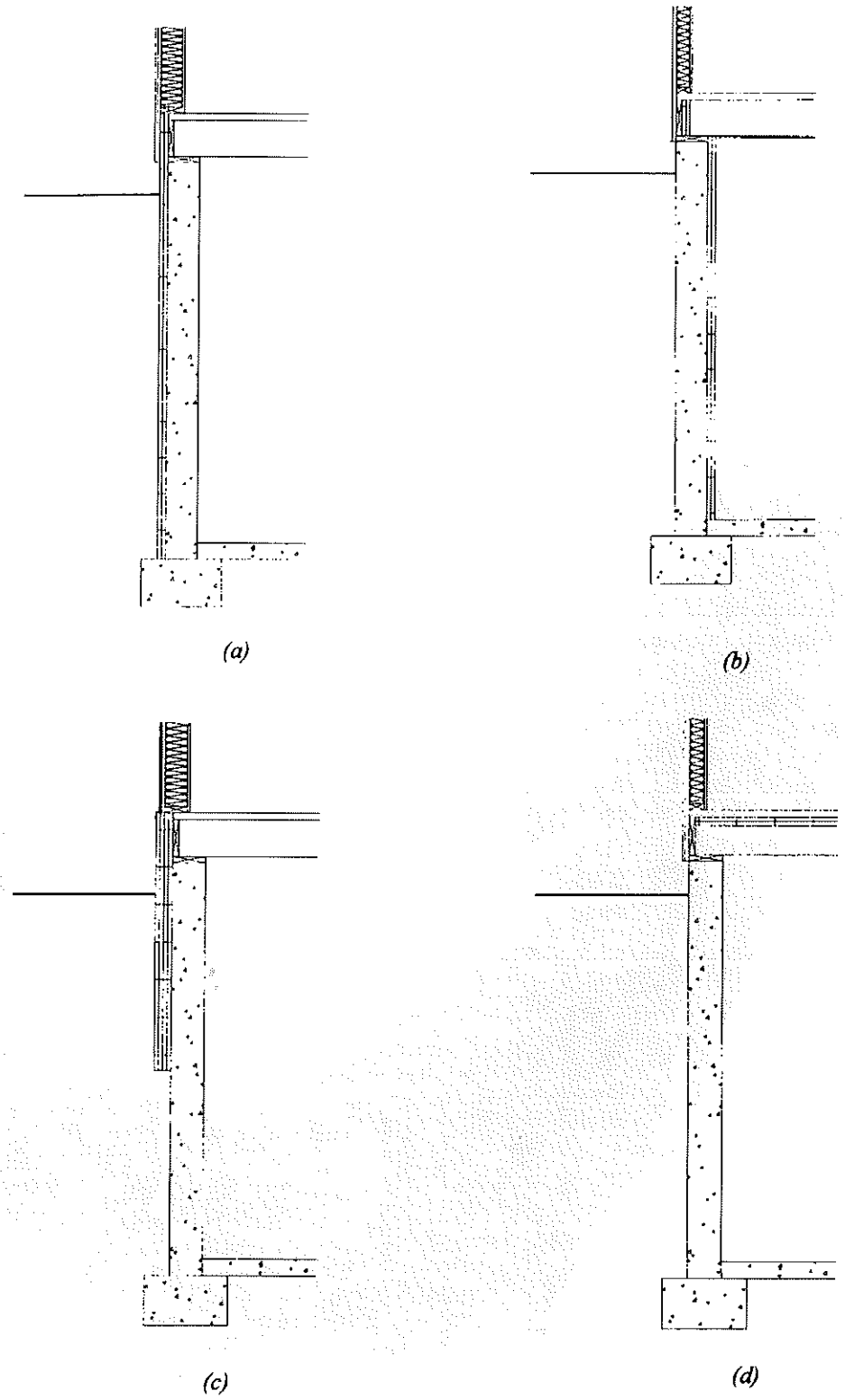

Figure 1 *Basement insulation configurations: a) full-height exterior insulation, b) full-height interior insulation, c) partial-height exterior insulation, d) ceiling insulation.*

energy required to maintain the air temperature in the basement within limits defined by heating and cooling setpoints. For unconditioned basements, the annual loads are credits and penalties for heating and cooling of the above-ground portion of the house by the basement. In other words, heat transfer through the basement ceiling adds or subtracts from above-ground conditioned space loads if outdoor temperature is outside the dead-band.

It was found that the unconditioned basement air temperature frequently is below the summer setpoint temperature. Conditioning of the basement is not required when this is the case. To account for this possibility, the air temperature of a conditioned basement is calculated by heat balance whenever outdoor air temperature exceeds the heating balance point temperature. If the calculated air temperature is less than the summer setpoint temperature during a given hour and the mechanical space conditioning system is in cooling mode, then the basement is not conditioned during that hour.

Computational Domain

A typical residential basement creates a thermal disturbance extending a substantial distance into the surrounding soil. In order to obtain an accurate estimate of basement heat loss, it is necessary to model not only the foundation, but also a portion of the surrounding soil sufficient to contain this disturbance. It has been shown (Bahnfleth 1989) that effects due to the asymmetry of solar radiation on foundation heat transfer are relatively small; therefore, the computational domain can be reduced in size through the application of symmetry conditions. Because of their disproportionate effect on heat transfer, the rim joist and the sill plate must also be modeled.

Energy Transport in Soil

Heat transport in the soil is a complex process that may include radiation, advection, and conduction. However, not all modes are significant for all soil types, moisture content levels, and temperature ranges. For example, radiative heat transfer within the voids of the soil matrix is significant only in dry soils at high temperatures (Sterling et al. 1993). Conduction is generally considered the predominant mode.

Advective heat transfer occurs in both the liquid and gaseous phases. Bligh and Smith (1983) found the influence of water infiltration to be short term and the moisture content of soil adjacent to building foundations to be close to field capacity most of the year. (Field capacity is the root zone water content of soil after being thoroughly wetted and allowed to drain for two days.) Thermally driven moisture migration is less significant than infiltration and, under typical field conditions, its effect on heat transfer is quite small when compared to conduction (Harlan and Nixon 1978). An investigation of transient, coupled, two-dimensional heat and moisture flow in the soil adjacent to a basement wall by Shen and Ramsey (1988) found negligible difference between coupled and uncoupled heat and mass transfer models for fine-grained soils such as clay. In an earlier study, Eckert and Pfender (1978) found thermally driven moisture flow to be negligible under the influence of the relatively small temperature gradients that typically exist in the soil near a building. In general, the advective transport mechanism in the ground around earth-sheltered buildings contributes insignificantly to the total heat flux and is neglected in this study.

Soil thermal conductivity is a function of temperature. However, for fine-grained soils, this temperature dependence is not pronounced (Sterling et al. 1993) and can be ignored at temperatures above 32°F (0°C) (Harlan and Nixon 1978). The potential for variation in soil thermal conductivity with moisture content is much more significant. However, Sterling et al. concluded in the above-referenced study that "one can seldom justify the expenditure of the resources necessary to measure or provide a detailed estimate of soil thermal conductivity solely for the purposes of optimizing insulation configuration for energy conservation." In other words, typical values rather than a detailed model should be sufficient.

On the basis of the findings noted above, the heat transfer model employed in the present basement simulation treats soil as a homogeneous medium having constant thermal properties. The net effect of all mechanisms of heat transfer is represented by an "apparent" thermal conductivity. It may be useful to think of apparent conductivity as analogous to eddy viscosity, which aliases all shear stress to the gradient of mean velocity in a turbulent flow. In the simulations described in this paper, apparent thermal conductivities of 0.64 Btu/h·ft·°F (1.1 W/m·K) and 1.1 Btu/h·ft·°F (1.9 W/m·K), respectively, for clay soil and gravel drainage bed were taken from the database compiled by Sterling et al. (1993).

Governing Equation, Boundary and Initial Conditions

Because heat and mass transfer are weakly uncoupled, the distributions of temperature (T) in the soil and in the basement walls and floor are governed, to a first approximation, by the three-dimensional heat conduction equation:

$$\rho c_p \frac{\partial T}{\partial t} = \frac{\partial}{\partial x}\left(k\frac{\partial T}{\partial x}\right) + \frac{\partial}{\partial y}\left(k\frac{\partial T}{\partial y}\right) + \frac{\partial}{\partial z}\left(k\frac{\partial T}{\partial z}\right) \quad (1)$$

where ρ is density, c_p is specific heat, k is thermal conductivity, t is time, and x, y, and z are, respectively, the south, west, and vertical coordinates. This form of the heat equation is applicable to the case of spatially variable soil properties, but in the present study, constant soil properties have been assumed. Boundary conditions must be provided for Equation 1 at

- interior surfaces of the basement and above the basement ceiling,
- above-ground exterior basement surfaces,
- the ground surface,

- "far-field" boundaries remote from the basement at which undisturbed soil conditions exist, and
- the "deep-ground" boundary at the lower limit of the computational domain.

Interior Surfaces. Interior surfaces may exchange heat by both convective and radiative processes. For a typical interior basement surface "i," the net heat flux into the surface (q_i) is given by

$$q_i = h_i(T_{room} - T_i) - q_{rad,i} \quad (2)$$

where h_i is the inside surface conductance, T_{room} and T_i are, respectively, the basement air temperature and the interior surface temperature of surface i, and $q_{rad,i}$ is the net radiative heat loss from the surface. Prior models have typically neglected the effects of radiation. However, Richmond and Besant (1985) have reported that surface radiation in an interior insulated, conditioned basement typically increases floor heat loss by 13% while decreasing wall heat loss by roughly 7% relative to the predictions of models using combined convection/radiation coefficients.

Inside surface, convection-only conductances were computed using a standard algorithm (ASHRAE 1975). Depending upon whether the basement is unconditioned, conditioned and within the dead-band, or conditioned and outside the dead-band, T_{room} is determined by heat balance or is equal to the setpoint. The radiative heat flux leaving each surface ($q_{rad,i}$) is calculated by a diffuse gray enclosure algorithm with emissivities of 0.9 for all surfaces. For the purpose of estimating the radiative flux distribution, interior foundation wall surfaces are divided into equally sized upper and lower regions, while the floor and ceiling are not subdivided. In principle, each interior finite-difference cell surface may be a distinct radiative surface. The need for vertical resolution should be greatest for uninsulated cases and diminish as insulation is added and interior wall temperature becomes more uniform.

For the special case of the basement ceiling, T_i is coupled to the above-ground indoor air temperature. As described previously, this temperature is assumed to be held at high and low limits for cooling and heating by the space conditioning system when outdoor temperature is outside the dead-band range and is assigned an intermediate value by interpolation when outdoor temperature is within the dead-band. The ceiling is represented by the thermal properties of the first story flooring (i.e., ρ equals 19.45 lb/ft^3 [311.7 kg/m^3] and c_p equals 0.36 Btu/lb·°F [1.5 kJ/kg·K]) with the ceiling joists and insulation modeled as a pure thermal resistance added to the underside of the flooring and calculated assuming parallel heat flow paths.

Above-Ground Exterior Basement Surfaces. The above-ground portion of the foundation wall is a vertical surface that experiences radiative and convective heat transfer. The expression for the surface heat flux (q_i) is similar to that given in Equation 2 for an interior surface:

$$q_i = h_i(T_{db} - T_i) - q_{rad,i} \quad (3)$$

The convective component of this flux is a function of the outside surface conductance (h_i) and the difference in outside air and surface temperatures (i.e., $T_{db} - T_i$). Like the interior surface conductance, h_i is calculated according to an algorithm widely used in energy calculations (ASHRAE 1975). The net radiative surface heat flux ($q_{rad,i}$) is equal to the sum of absorbed solar radiation (direct, diffuse, and reflected) and infrared sky radiation less emitted infrared surface radiation. An algorithm was developed to determine these values from hourly TMY weather files (NOAA 1979) that give the normal direct and diffuse solar radiation received on a horizontal surface during the preceding 60 minutes. The mathematical representation of diffuse solar radiation incident on a vertical surface is presented in ASHRAE (1975) and McQuiston and Parker (1994), while the incoming sky radiation is computed by means of Angstrom's empirical clear-sky correlation (Geiger 1961). The infrared radiation reflected from the ground surface is a function of the ground-surface cover as represented by the surface albedo value of 0.16 or 0.40, respectively, for grass and snow (Kung et al. 1964).

Ground Surface. A complex energy balance between conduction, convection, radiation, and evapotranspiration takes place at the ground surface. The ground-surface boundary condition employed in the present model includes all of these components and has the form given by Sellers (1965):

$$G = R_t - q_{cs} - q_{et} \quad (4)$$

where G is conduction into the ground, R_t is the net solar and infrared radiation absorbed at the ground surface, q_{cs} is convection at the surface, and q_{et} is evapotranspiration.

Evaluation of Equation 4 follows the procedure used by Speltz and Meixel (1981) in their study of earth-covered roofs. Above-ground climatic data are taken from TMY weather files (NOAA 1979). The fraction of incident radiation absorbed at the ground surface is a function of the amount of direct and diffuse solar radiation incident on a horizontal surface and the radiative properties of the ground surface. The model permits variation in surface albedo between grass and snow-covered values. The sensible convective heat flux is proportional to the temperature difference between the ground surface and the air. Evapotranspiration accounts for all latent heat exchange at the ground surface, including evaporation and convection of water from the soil surface and transpiration by plants. The actual rate of evapotranspiration depends on both meteorological conditions and the supply of moisture to the ground. However, the condition of saturated soil has been found to closely represent actual conditions that would exist for a typical lawn (Sterling et al. 1993). As a matter of convenience, it was assumed that the soil is saturated and evapo-

transpiration proceeds at its potential (maximum) rate, which is more easily estimated.

Far Field. At a large distance from the foundation, the disturbance created by the ground temperature distribution becomes negligible. A sensitivity study by Shipp et al. (1981) indicated that little or no change in predicted heat loss occurs when the far-field boundary is at least 39.4 ft (12 m) away from the building. Therefore, their model applied a zero lateral flux boundary condition at this distance from the foundation perimeter. In the present model, a specified temperature boundary condition is applied at the perimeter of the domain. The imposed temperatures are calculated by a one-dimensional implicit finite-difference solution with a fixed deep-ground temperature and a ground-surface heat balance boundary condition as previously described.

Deep Ground. Depending upon groundwater conditions, either zero flux or fixed temperature conditions may be appropriate along the lower boundary of the domain. A zero flux boundary is an accurate representation of reality when the water table is deep. When the water table is relatively near the ground surface, a fixed temperature condition may be more representative. However, extensive analyses of earth temperature data from 63 weather stations throughout the United States by Kusuda and Achenbach (1965) indicated that the annual average earth temperature at 30 ft to 60 ft (9.1 m to 18.3 m) depth is essentially constant and equal to the average annual ground-surface temperature, but it can be approximated by the average annual air temperature. This approximation has been adopted in the present model.

Initial Condition. Because a steady-periodic solution is desired, the choice of initial condition is arbitrary; however, a poor choice could increase the number of annual iterations needed to achieve convergence. In the present case, the entire domain was initialized to the undisturbed soil temperature distribution existing at the first hour of the simulation.

Numerical Method

Equation 1 was solved by an improved alternating-direction-implicit (ADI) finite-difference numerical method (Chang et al. 1991). The improved method allows use of a larger time step while retaining stability and accuracy. Compared to conventional ADI algorithms, such as those of Brian (1961) and Douglas (1962), this method has greater accuracy and requires less computer storage (Chang et al. 1991). The domain was discretized using the control volume approach (Patankar 1980). Figure 2 shows a cross section of the domain. The variable grid is refined in areas that experience large temperature gradients, such as along the ground surface and near the foundation.

Minimum cell dimensions near the foundation wall were based on studies by Meixel et al. (1979) and Shipp et al. (1981) that found grid spacing less than 11.8 in. (0.3 m) and 3.9 in.

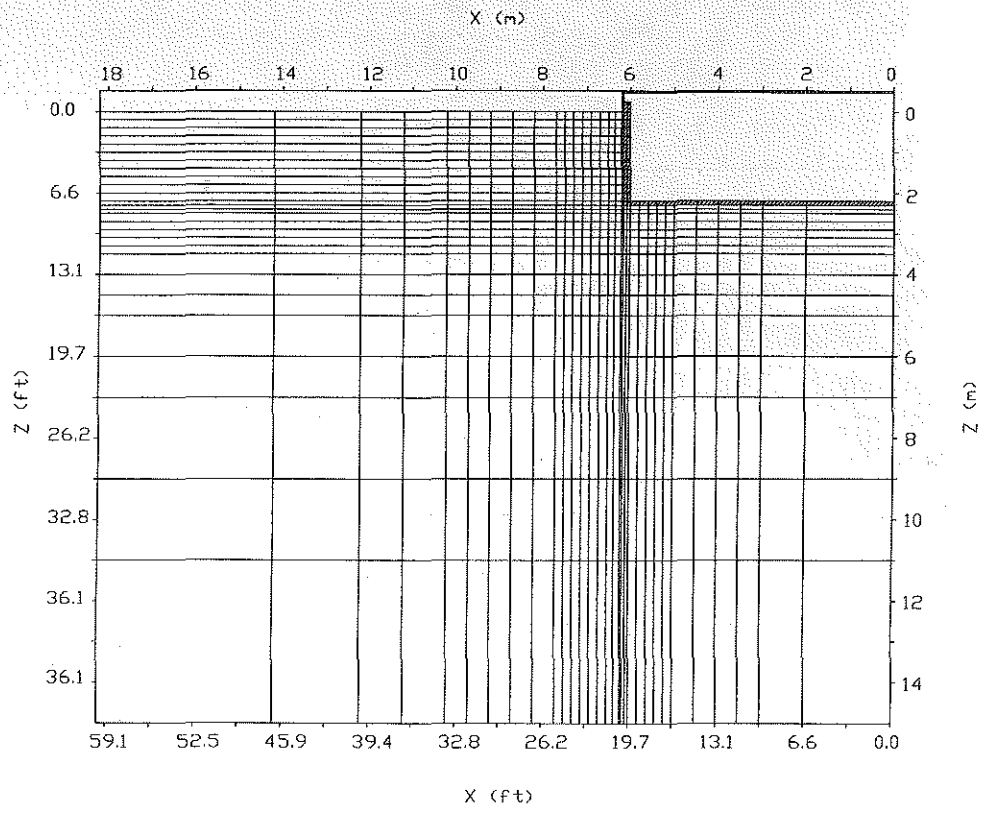

Figure 2 *Vertical section of finite-difference grid.*

(0.10 m), respectively, around the structure acceptable for achieving accurate results. In addition, minimum cell dimensions were established in accordance with the accuracy and stability criteria set forth by the numerical method employed in the study. Grid spacing in the present model in the vicinity of the building foundation ranged from 3.9 in. (0.1m) to 7.8 in. (0.2 m), while spacing at far-field and deep-ground boundaries was as great as 6.5 ft (2 m). For this grid, simulations using an hourly time step required four to ten hours of execution time on PCs of varying capability. The elapsed simulated time required for convergence was typically three to five years. It is expected that substantial reductions in this execution time can be realized by employing longer time steps in portions of the domain that are not strongly influenced by variations in conditions on such a short time scale. This will make the model of more practical use when coupled with a whole-building program.

VALIDATION

The current model (Base3D) was validated (albeit not extensively at this point) against BASECALC (CANMET 1995), which is based on the Mitalas method (Mitalas 1982). Validation study parameters (Table 1) were selected to match limitations in the capabilities of BASECALC in order to permit a direct comparison. For the purpose of validation, Base3D was modified to maintain a constant basement air temperature and to use combined convection/radiation surface conductances in place of the surface radiation model. Heat transfer through the sill box was neglected.

TABLE 1
Model Parameters for Validation Study

Depth of foundation wall below grade	7.2 ft (2.2 m)
Height of foundation wall	7.9 ft (2.4 m)
Width of basement	39.4 ft (12 m)
Length of basement	39.4 ft (12 m)
Foundation wall thickness	7.9 in. (0.2 m)
Foundation wall conductivity	0.81 Btu/h·ft·°F (1.4 W/m·K)
Floor slab thickness	3.9 in. (0.10 m)
Floor slab conductivity	0.81 Btu/h·ft·°F (1.4 W/m·K)
Insulation R-value	0 h·ft^2·°F/Btu (0 m^2·K/W)
Climatic site	Allentown, Pa.
Average ground surface temperature	50.9°F (10.5°C)
Annual amplitude	23.4°F (12.8°C)
Soil thermal conductivity, above-floor slab	0.64 Btu/h·ft·°F (1.1 W/m·K)
Soil thermal conductivity, below-floor slab	0.64 Btu/h·ft·°F (1.1 W/m·K)
Water table depth	49.2 ft (15 m)
Basement air temperature	69.8°F (21°C)

In Figure 3, monthly average foundation wall and floor slab heat losses for an uninsulated, conditioned basement predicted by BASECALC are compared with results from Base3D with modified parameters to match BASECALC and with the assumption used in the current model, which includes the sill box and surface radiation models and accounts for dead-band operation.

When model parameters match, agreement between Base3D and BASECALC is very good. Monthly heat loss estimates differ by –0.4% to 14%. Annual heat loss varies by approximately 6%, with the current model predicting higher losses than BASECALC. When more realistic conditions are considered, the current model yields considerably lower values (–45%) than BASECALC. Although the sill box and surface radiation act to increase basement heat loss, the dead-band operation significantly reduces the indoor/outdoor air temperature difference for much of the year. An uninsulated, conditioned basement in Allentown, Pennsylvania, for example, is in dead-band mode for almost 50% of the hours during a typical year.

CASE STUDY

In order to illustrate the capabilities of the model, several insulation strategies were investigated for a conventional cast-in-place concrete basement located in Allentown, Pennsylvania, for both conditioned and unconditioned scenarios. The computational domain consisted of one quadrant of a 39.4 ft by 39.4 ft (12 m by 12 m) rectangular basement and the surrounding soil. The foundation wall was 8 in. (0.2 m) wide by 8 ft (2.4 m) tall with 8 in. (0.2 m) exposed above grade. The horizontal and vertical limits of the domain were located 39.4 ft (12 m) from the foundation wall and 49.2 ft (15 m) below grade, respectively. The gravel drainage bed extended 4 in. (0.1 m) below the floor slab and 12 in. (0.3 m) beyond the foundation wall to a total depth of 16 in. (0.4 m). The minimum basement air temperature for heating was set to 69.8°F (21°C) and the maximum temperature for cooling was set to 77.0°F (25°C). Dead-band temperature limits were assumed to be 48°F (8.9°C) and 72°F (22.2°C). These values were based on heating and cooling balance points determined from the results of simulations of a 1500 ft^2 (139.4 m^2) house in several Pennsylvania locations (Werling 1994). Annual heating and cooling hours for a particular site were correlated with hourly weather data to determine the temperatures above and below which mechanical cooling and heating systems operate. The limiting dead-band temperature for heating was compared with that from a field study of single-family residences in central Pennsylvania (Yuill and Musser 1997). The deep

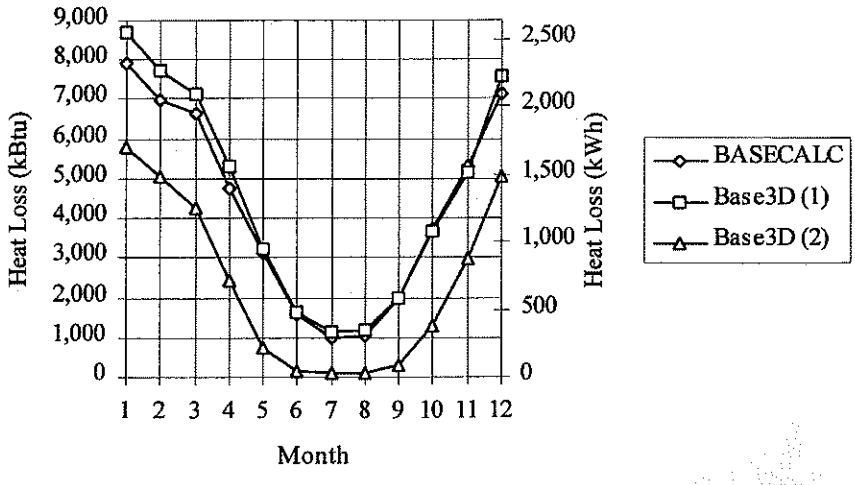

Figure 3 *Comparison of monthly total heat loss with BASECALC. (1) Base3D parameters modified to match BASECALC assumptions. (2) Base3D unmodified.*

ground temperature was set equal to 50.9°F (10.5°C) at a depth of 49.2 ft (15 m) below grade.

Six simulations were performed. For conditioned basements, four insulation configurations were modeled: uninsulated, full-height interior wall insulation of 2 in. (51 mm) extruded polystyrene insulation board (XPS) having a thermal resistance of R-10 (1.76 m^2·K/W), full-height R-10 (1.76 m^2·K/W) XPS exterior wall insulation, and partial-height exterior insulation in which the upper half of the foundation wall was covered with R-20 (3.52 m^2·K/W) XPS. Because the same type and amount of insulation was used in each case, differences between cases should be due to the effect of insulation location. For the unconditioned basement, two configurations were investigated: uninsulated and R-10 (1.76 m^2·K/W) XPS ceiling insulation.

Energy consumption and cost were calculated for two common residential space heating and cooling systems: a natural gas-fired furnace/direct expansion air-conditioner combination (DX A/C) and an electric air-source heat pump (ASHP). Equipment performance factors reflect seasonal energy-efficiency requirements presented in the *Model Energy Code* (CABO 1995). Energy prices for Allentown were determined from monthly average residential data published by the Pennsylvania Public Utility Commission (1996a, 1996b, 1997a, 1997b).

RESULTS

Annual Performance

Table 2 summarizes annual basement energy usage and Table 3 summarizes annual energy cost results. In the case of a conditioned basement, a heating or cooling load is the actual energy required to maintain the desired air temperature in the basement. For an unconditioned basement, heating and cooling loads are actual loads on the above-ground portion of the building due to heat transfer through the basement ceiling.

For the Allentown climate, annual basement heating loads are substantially larger than cooling loads. This can be attributed to the large heating season temperature difference between the indoor air and the ground and the tendency of the ground to remain cooler than the indoor setpoint temperature during the cooling season. Because the ground is generally cooler than the basement interior, below-grade walls tend to lose heat to the surrounding soil in the summer even when the outdoor air temperature is quite warm and there is net heat gain through the above-ground foundation wall and sill box. In the uninsulated case, the net effect of the basement was to reduce building cooling load, so the effect of adding insulation was generally to decrease this benefit. Therefore, savings associated with insulation were due entirely to heating load reductions. For all cases, the effect of insulation in this climate was to reduce the sum of annual basement heating and cooling loads and to reduce annual basement-related energy cost.

Conditioned Basements. Relative to the uninsulated case, full-height exterior insulation reduced the heating load by 48%, or 13,006 kBtu (3,812 kWh) relative to the uninsulated case, while the cooling load increased by 188%, or 689 kBtu (202 kWh). Interior insulation over the full height of the foundation wall and sill box reduced the basement heating load by 52%, or 14,121 kBtu (4,139 kWh) and reduced the cooling load by 8%, or 28 kBtu (9 kWh). The exterior placement of the thermal mass relative to insulation damps the effects of thermal variations and solar radiation on exposed surfaces while producing colder soil temperatures surrounding the basement. Compared to the other cases, this results in lower surface temperatures and a lower basement air temperature as calculated during dead-band operation; however, cooling load differences of this magnitude are of no real significance compared to the heating load. If the foundation wall is insulated over its full height, predictions of basement heating loads differed by approximately 4%, or 1,115 kBtu (327 kWh) between exterior and interior insulation placement. This result

TABLE 2
Annual Performance Summary—
Energy Loads and Equipment Energy Consumption, Allentown, Pa.

Case	Seasonal Energy Loads, kBtu (kWh)				Seasonal Energy Consumption					
	Heating Load	Δ %	Cooling Load	Δ %	Winter Furnace	Summer DX/A/C	Total	Winter ASHP	Summer ASHP	Total
Conditioned										
Uninsulated*	26,905 (7,886)	–	−366 (−107)	–	34,494 (10,110)	−125 −37	34,369 (10,074)	17,803 (5,218)	−129 (−38)	17,674 (5,180
Full-Height Exterior	13,899 (4,074)	−48.3	323 (95)	−188.2	17,819 (5,223)	110 (32)	17,930 (5,255)	9,197 (2,696)	114 (33)	9,310 (2,729
Full Height Interior	12,784 (3,747	−52.5	−-394 (−116)	7.6	$16,389 (4,804)	−134 (−39)	16,255 (4,764)	8,459 (2,479)	−139 (−41)	8,320 (2,439)
Partial-Height Exterior	18,035 (5,286)	−33.0	111 (32	−130.3	23,122 (6,777)	38 (11)	23,160 (6,788)	11,934 (3,498)	39 11	11,973 (3,509)
Unconditioned										
Uninsulated	3,986 (1,168)	–	−451 (−132)	–	5,110 (1,498)	−154 (−45)	4,956 (1,453)	2,637 (773)	−159 (−57)	2,479 (726)
Ceiling	3,412 (1,000)	−14.4	−536 (−157)	18.8	4,374 (1,282)	−183 (−54)	4,191 (1,228)	2,258 (662)	−189 (−55)	2,069 (606)

* Base case.

is consistent with a previous study using a two-dimensional model, which predicted less than 10% difference in heating season heat loss between exterior and interior placement for equivalent amounts of R-10 (1.76 m^2·K/W) insulation (Shipp and Broderick 1983).

The difference in performance between full and partial exterior insulation with the same total R-value was greater than the difference between interior and exterior full-height insulation. Full-height exterior R-10 (1.76 m^2·K/W) insulation reduced conditioned basement energy consumption by 48% relative to the uninsulated case, while partial-height R-20 (3.52 m^2·K/W) produced a reduction of approximately 33%. This confirms that it is better to distribute a given amount of insulation over the full height of the wall rather than concentrating it near the surface.

Unconditioned Basements. Results for the unconditioned case show a modest reduction in annual heating and cooling season energy consumption of 14% and 19%, respectively, when insulated between the floor joists. While the change in seasonal energy consumption is greater for cooling than for heating, the overall heating load for the insulated case is six times that of the cooling. These changes, it should also be noted, are relative to an uninsulated base energy consumption that is smaller by a factor of eight than the conditioned uninsulated case.

Table 3 shows that the energy cost impact of an unconditioned basement is small, even in the uninsulated case. In the worst case, heat transfer through the ceiling added less than $75 per year to the total house energy cost. While annual energy savings associated with adding R-10 (1.76 m^2·K/W) insulation to a conditioned basement were $100 to $300, adding R-10 (1.76 m^2·K/W) to the ceiling of an unconditioned basement saved only $10 to $50 annually depending on the type of heating and cooling equipment. These small savings make it difficult to justify ceiling insulation for this particular climate on the basis of economics. However, ceiling insulation has other benefits, for example, warmer floor temperatures in the adjacent occupied above-ground space.

Basement Heat Transfer Characteristics

Conditioned Basements. Conditioned basement interior wall surface heat flux distributions on the 21st day of the peak heating month (February) and the 21st day of the peak cooling month (July) are shown in Figures 4 and 5. During winter conditions, a high flux region exists just below the intersection of the foundation wall and the grade line, as evidenced by the compression of the heat flux contours at this location. For the case of full-height exterior insulation, high flux regions also exist near the intersection of the wall and floor slab and at the sill box. During summer conditions, differences in heat flux profiles are hardly discernible due to a substantial decrease in basement heat loss as a result of a much smaller driving potential. A significant vertical component to the heat flux gradient exists for all cases along the upper half of the wall section, except for interior insulation where it appears over the wall's full height.

TABLE 3
Annual Performance Summary— Energy Cost, Allentown, Pa.

Case	Seasonal Energy Cost, $					
	Winter Furnace	Summer DX/AC	Total	Winter ASHP	Summer ASHP	Total
Conditioned						
Uninsulated	338	–3	335	437	–3	434
Full-Height Exterior	175	3	178	226	3	229
Full-Height Interior	161	–4	157	208	–4	204
Partial-Height Exterior	227	1	228	293	1	294
Unconditioned						
Uninsulated	50	–4	46	65	–4	61
Ceiling	43	–5	38	55	–5	51

TABLE 4
Heat Loss per Unit of Perimeter Length, 21 January, Allentown, Pa.

	Total	Rim Joist		Sill Plate		Foundation Wall		Floor Slab	
	Btu/ft (W-h/m)	Btu/ft (W-h/m)	% of Total	Btu/ft (W-h/m)	% of Total	Btu/ft (W-h/m)	% of Total	Btu/ft (W-h/m)	% of Total
Conditioned									
Uninsulated	1095 (1053)	77 (74)	7.0	59 (57)	5.4	809 (778)	73.8	151 (145)	13.8
Full-Height Exterior	655 (630)	50 (48)	7.6	26 (25)	4.0	470 (452)	71.8	109 (104)	16.6
Full-Height Interior	542 (521)	39 (37)	7.1	29 (28)	5.4	371 (356)	68.4	103 (99)	19.0
Partial-Height Exterior	867 (833)	35 (33)	14.3	23 (22)	2.7	668 (642)	77.0	141 (136)	16.3
Unconditioned									
Uninsulated	207 (199)	30 (28)	14.3	30 (29)	14.3	285 (274)	137.6	–137 –(132)	–66.2
Ceiling	157 (151)	10 (10)	6.4	6 (6)	4.0	268 (258)	171.4	–128 (123)	–81.8

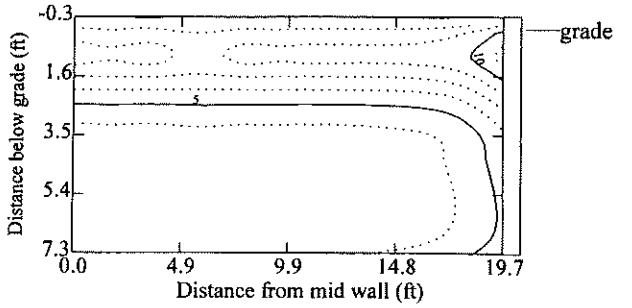

(a)

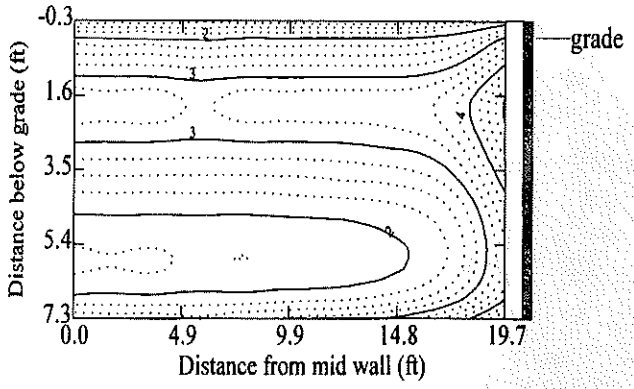

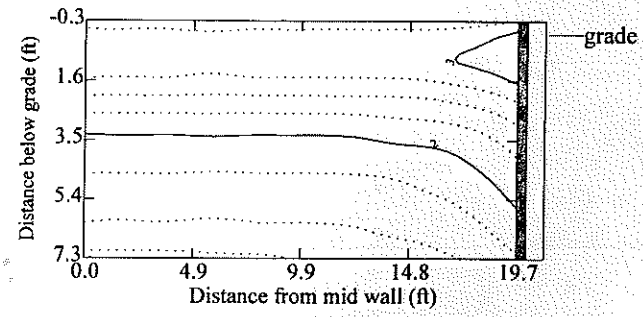

(c)

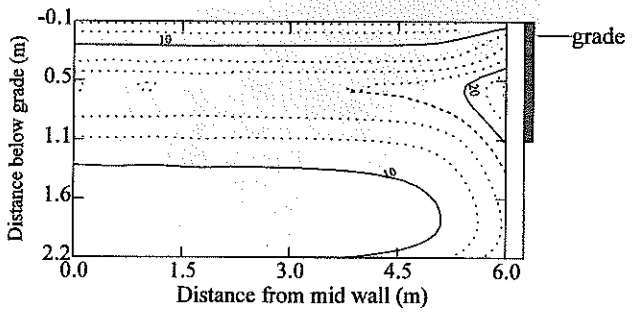

(d)

Figure 4a *Conditioned basement wall heat flux, 21 February, Btu/h·ft², Allentown, Pa:. a) uninsulated, b) full-height exterior insulation, c) full-height interior insulation, d) partial-height exterior insulation.*

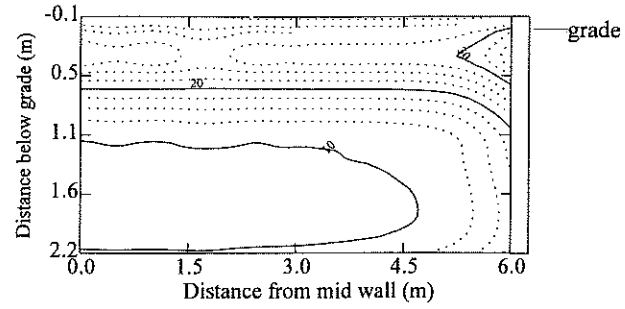

(a)

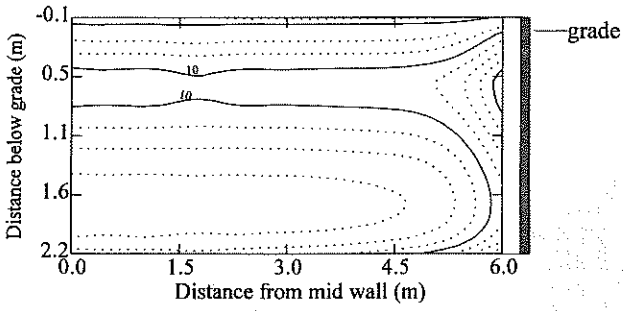

(b)

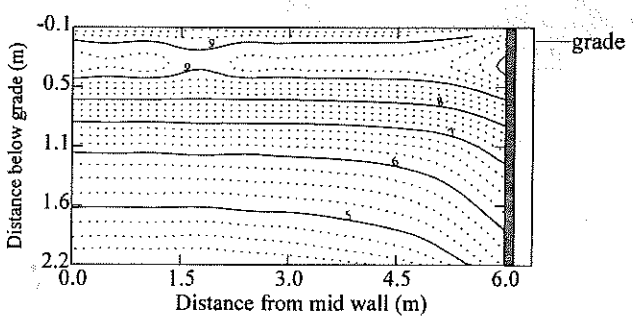

(c)

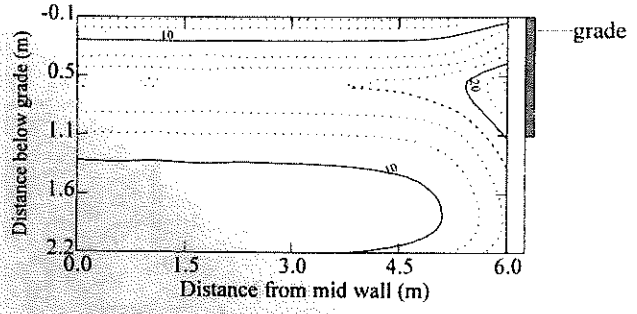

(d)

Figure 4b *Conditioned basement wall heat flux, 21 February, W/m^2, Allentown, Pa.: a) uninsulated, b) full-height exterior insulation, c) full-height interior insulation, d) partial-height exterior insulation.*

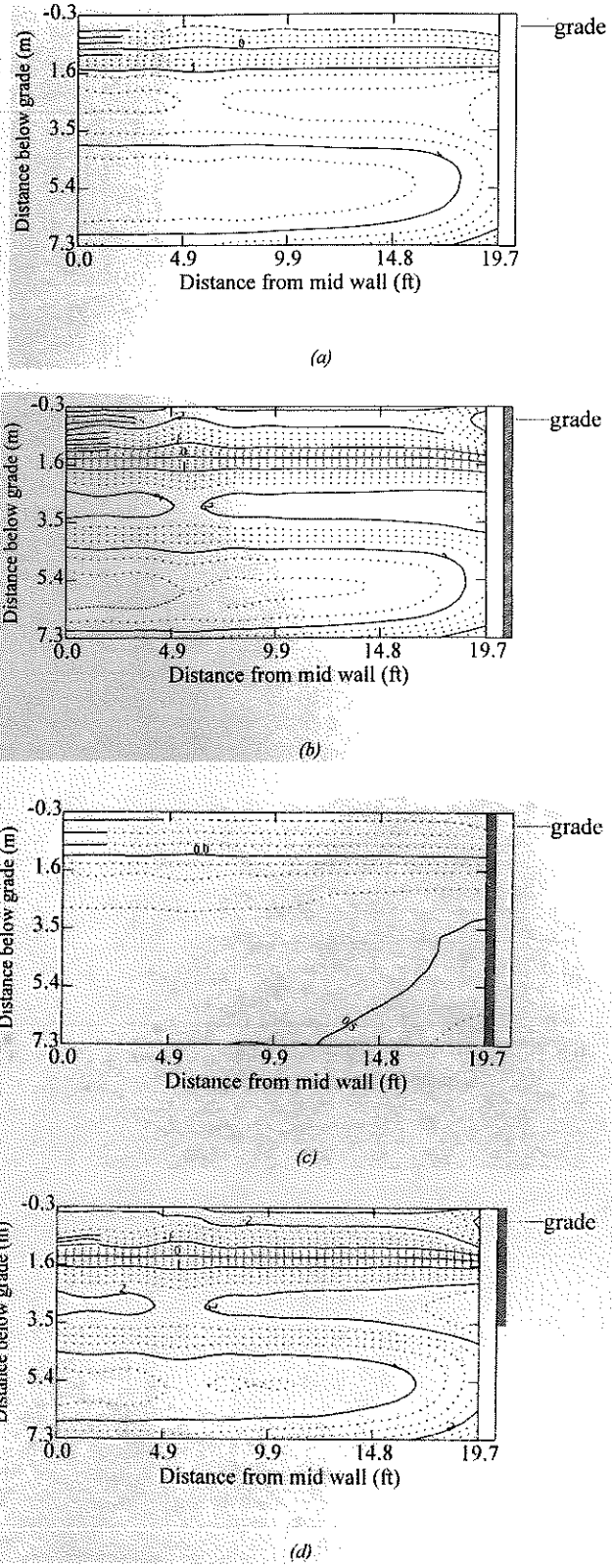

Figure 5a *Conditioned basement wall heat flux, 21 July, Btu/h·ft^2, Allentown, Pa.: a) uninsulated, b) full-height exterior insulation, c) full-height interior insulation, d) partial-height exterior insulation.*

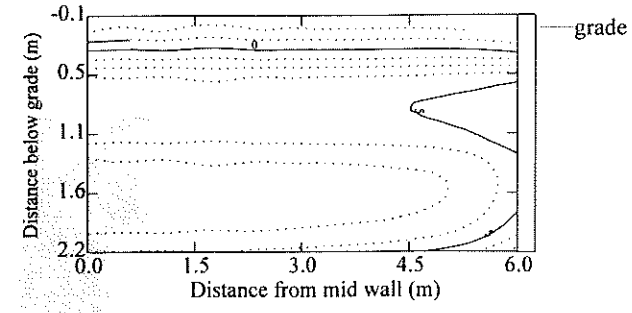

(a)

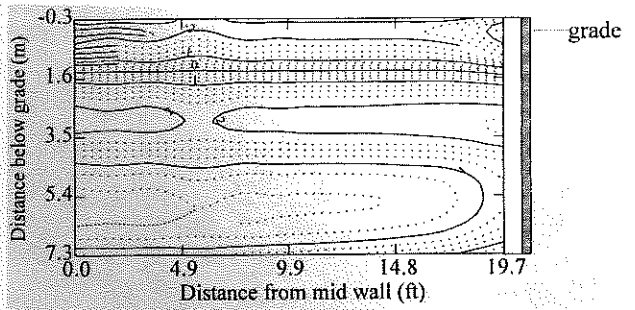

(b)

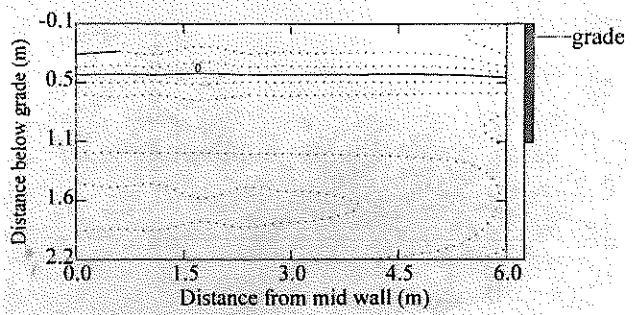

(d)

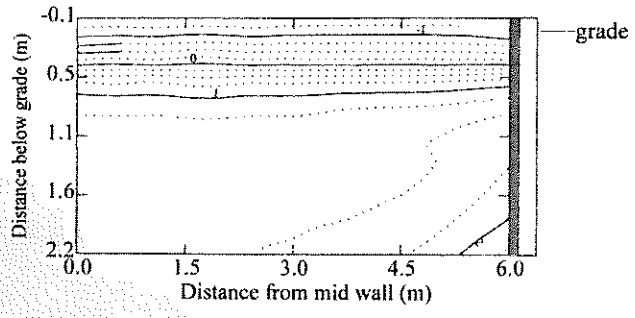

(c)

Figure 5b *Conditioned basement wall heat flux, 21 July, W/m^2, Allentown, Pa.: a) uninsulated, b) full-height exterior insulation, c) full-height interior insulation, d) partial-height exterior insulation.*

The contribution of each surface to the total basement heat loss is presented in Table 4 in terms of total and percent of total basement heat loss per unit perimeter length for January 21. Negative values indicate a net heat gain to the space. Solar loads can elevate rim joist temperatures above basement air temperatures for part of the day. The sill box (rim joist and sill plate) accounts for 10% to 12% of the total basement heat loss. These findings are consistent with those of Wang (1979), who estimated a 9% to 15% increase in seasonal heat loss from a conditioned basement sill box. This finding is significant given that most models of basement heat transfer have neglected the sill box.

The heat flux distribution over the height of the foundation can further be illustrated by plotting the horizontally averaged rim joist, sill plate, and wall heat fluxes per depth above and below grade for January 21 (Figure 6). The region of highest heat flux exists just below the intersection of the grade line and the foundation wall where vertical heat transfer occurs. A spike in the heat flux is also present at the rim joist and at the intersection of the wall and floor slab for all cases except full-height interior insulation, where two-dimensional heat transfer is diminished.

Figure 7, which shows vertically averaged wall heat fluxes for January 21, illustrates the effects of three-dimensional heat transfer. Corner effects are seen to influence the wall heat flux distribution up to a distance of approximately 5 ft (1.5 m) from the corner, which constitutes one-fourth of the modeled foundation wall. The area-averaged heat flux in this region is 20% greater than that of the center region for an uninsulated wall. Multi-dimensional effects can produce as much as 6% higher area-averaged foundation wall heat losses for a chosen day in January than would be indicated solely by center wall heat fluxes.

A similar effect occurs at the corners of the floor slab, as shown in Figure 8, where floor heat fluxes are plotted as a function of distance along a diagonal from a typical corner (i.e., flux is averaged over strips perpendicular to the diagonal). Three-dimensional effects primarily influence the area within 5 ft (1.5 m) of the corner. In the case of insulation applied to the inside surface of the foundation wall, temperatures can approach freezing at the grade line. Colder surface temperatures at the bottom of the foundation wall significantly increase floor slab heat loss at the corner. The floor slab temperature is also influenced by that of the ceiling, which radiates to it. As ceiling temperatures increase with the application of insulation, so do floor slab temperatures at a distance from the corner. The result is a large thermal gradient within the floor slab of as much as 15°F (8.6°C).

Figures 9 and 10 show typical winter and summer isotherms within the soil adjacent to an uninsulated conditioned basement. Winter results corroborate the conclusion of Latta and Boileau (1969) that isotherms extend radially from the intersection of the grade line and the foundation wall for an uninsulated basement and that heat flow paths are circular arcs normal to these isotherms. Theoretically, as insulation is applied, isotherms will approach horizontal lines and heat flow will become vertical (ASHRAE 1997). However, the addition of R-10 (1.76 $m^2 \cdot K/W$), as investigated in the current study, does not significantly alter the overall shape of the temperature profiles within the soil surrounding a basement.

The majority of the influence of adding insulation occurs within and immediately adjacent to the foundation wall. Both in the vicinity of the foundation wall as well as in the far field, marked changes in the ground temperature regime occur from season to season. As evidenced by horizontal isotherms at the far-field boundary, the building disturbs the soil temperature up to a distance of approximately 40 ft (12 m). During the winter, a high heat flux region occurs along the upper half of the foundation wall. In the summer, flux levels under the floor increase while those along the wall decrease. Isotherms under the floor become more horizontal.

Unconditioned Basements. When the basement is not directly heated or cooled to maintain a setpoint temperature, the resulting basement air temperature ranges between 49°F (9.4°C) and 73°F (22.8°C), while the first-story air temperature ranges between seasonal setpoint temperatures as shown in Figure 11. Applying insulation between the floor joists of the ceiling thermally isolates the basement from the above-ground space and results in colder indoor air and surface temperatures year-round. Although this has a beneficial effect in reducing the summer cooling load, as shown in Table 2, cold surface temperatures tend to render the basement uninhabitable and make it vulnerable to freezing in the winter.

As previously noted, floor slab surface temperatures are significantly influenced by the temperature of the ceiling that radiates to it. The floor slab is generally warmer than the basement air temperature and, thus, experiences a net heat gain. As insulation is applied to the ceiling, decreasing not only the ceiling temperature but the floor temperature as well, the relative change in basement air temperature results in an overall net reduction in the heating benefit of the floor slab.

Unconditioned basement interior wall surface heat flux distributions on the 21st day of the peak heating month (February) and the 21st day of the peak cooling month (July) are shown in Figures 12 and 13. Representative winter foundation wall heat flux profiles are similar in appearance to those for the conditioned, uninsulated case. A high heat flux region exists below the intersection of the foundation wall and the grade line, and a strong vertical component is present within the foundation wall. Accordingly, the foundation wall accounts for the majority of the heat loss within an unconditioned basement. Representative summer profiles are also similar in that a high heat flux region exists at the intersection of the floor slab and the foundation wall for both the uninsulated and ceiling insulated cases. The addition of ceiling insulation results in a heat gain through the upper 1.5 ft (0.5 m) of the foundation wall but a net basement heat loss overall.

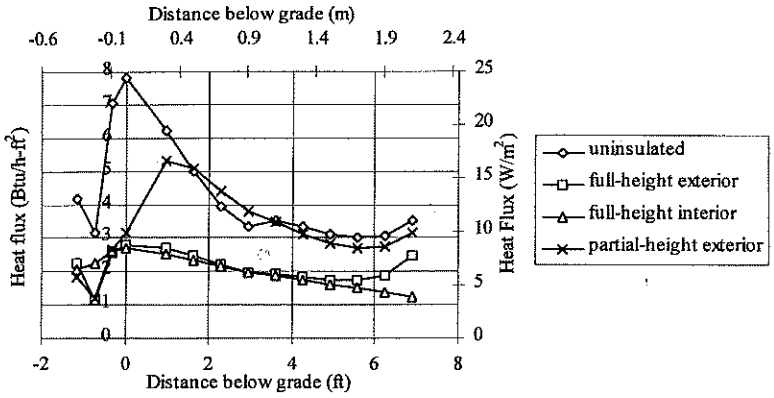

Figure 6 *Horizontally averaged wall and sill box heat fluxes, 21 January, Allentown, Pa.*

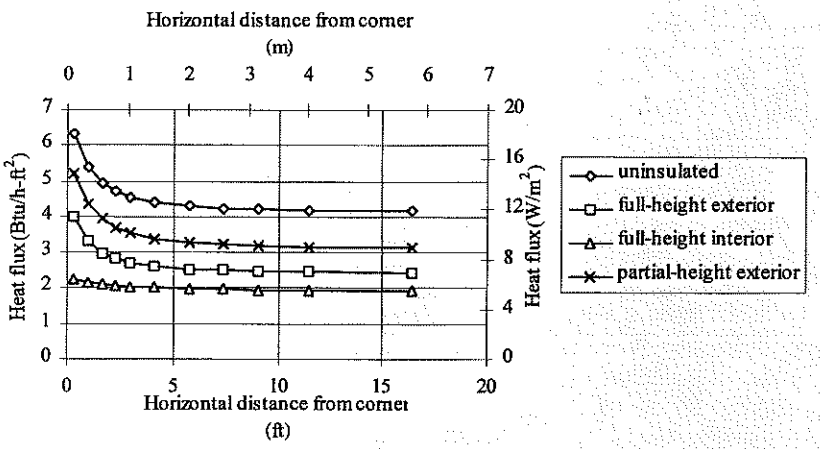

Figure 7 *Vertically averaged wall heat flux distribution for a conditioned basement, 21 January, Allentown, Pa.*

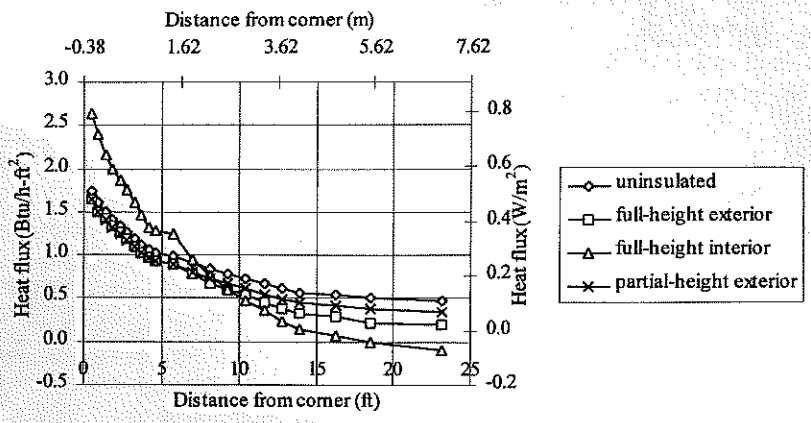

Figure 8 *Area-averaged floor heat flux distribution for a conditioned basement, 21 January, Allentown, Pa.*

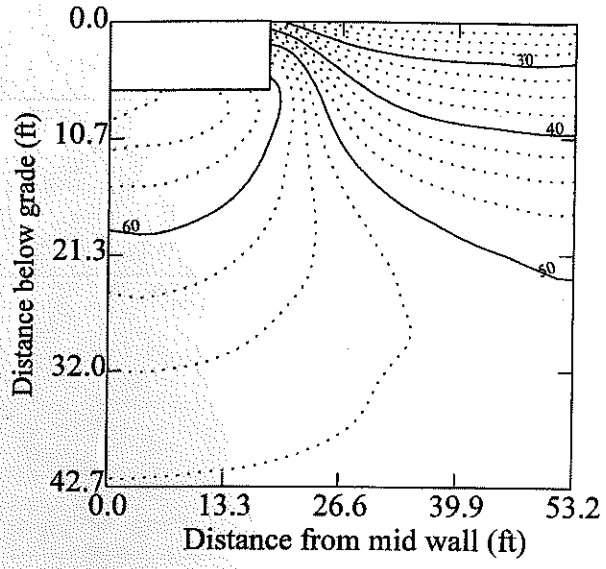

Figure 9a *Daily averaged soil isotherms (°F) for an uninsulated, conditioned basement, 21 February, Allentown, Pa.*

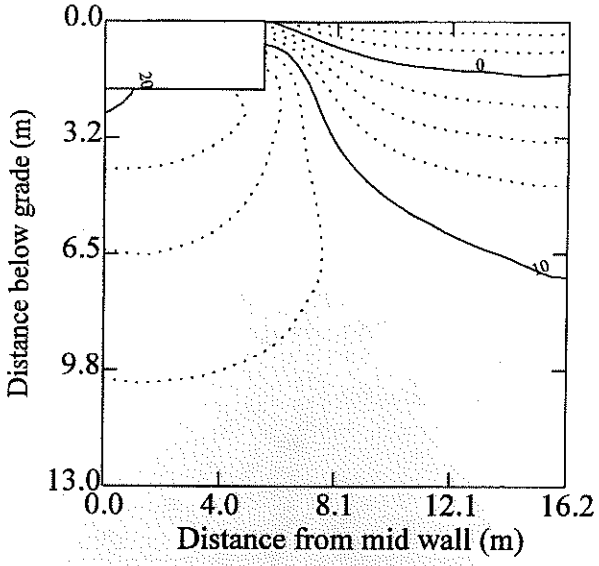

Figure 9b *Daily averaged soil isotherms (°C) for an uninsulated, conditioned basement, 21 February, Allentown, Pa.*

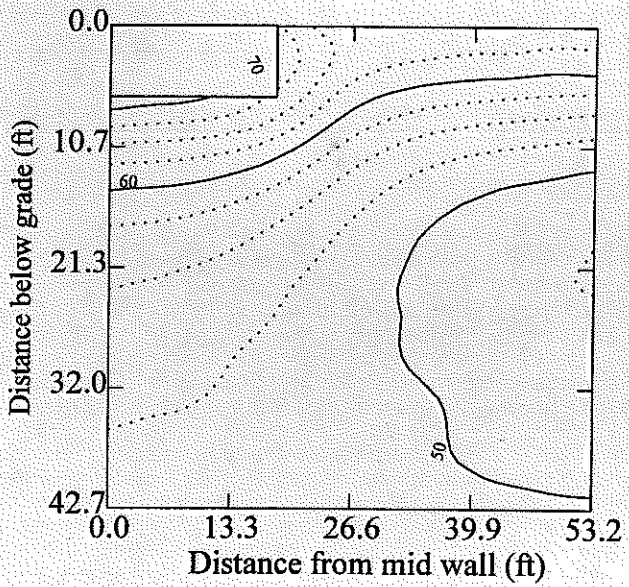

Figure 10a *Daily averaged soil isotherms (°F) for an uninsulated, conditioned basement, 21 July, Allentown, Pa.*

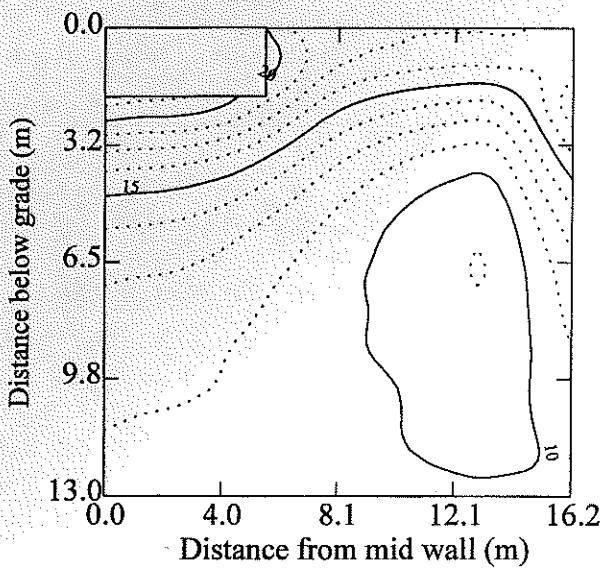

Figure 10b *Daily averaged soil isotherms (°C) for an uninsulated, conditioned basement, 21 July, Allentown, Pa.*

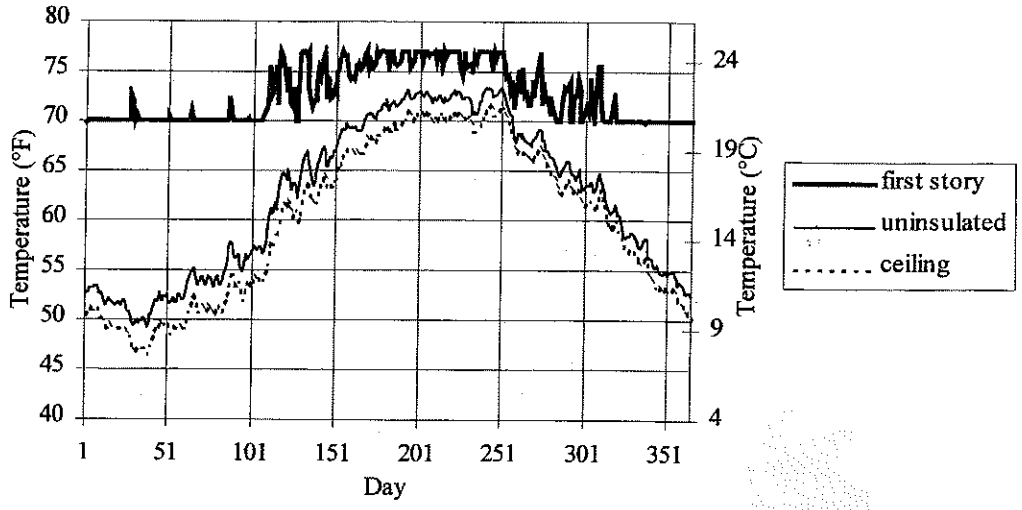

Figure 11 *Daily average first story and unconditioned basement air temperatures with and without ceiling insulation, Allentown, Pa.*

TABLE 5
Comparison of Model Results with Building Foundation Design Handbook (FDH, Labs et al. 1988)

	Heating and Cooling Loads, kBtu (kWh)						Energy Cost		
	FDH* —Whole House		Base3D†- Basement		% Whole Load				
	Heating	Cooling	Heating	Cooling	Heating	Cooling	FDH*	Base3D†	% of FDH Predicted
Conditioned									
Uninsulated, R-0	89,800 (26,320)	3,980 (1,167)	26,905 (7,886)	-366 (-107)	30.0	-9.3	$0	$0	0.0
Full-Height Interior, R-10	52,000 (15,241)	3,990 (1,169)	13,899 (4,074)	323 (95)	26.7	8.0	$314	$175	55.8
Full-Height Exterior	52,000 (15,241)	3,980 (1,167)	12,784 (3,747)	-394 (-116)	24.6	-9.8	$317	$170	53.7
Partial-Height Exterior, R-10	59,000 (17,556)	3,970 (1,164)	18,035 (5,286)	111 (32)	30.1	2.8	$243	$97	40.0
Unconditioned									
Uninsulated, R-10	62,000 (18,172)	3,490 (1,023)	3986 (1,186	-451 (-132)	6.5	-12.9	$0	$0	0.0
Ceiling, R-10	46,500 (13,629)	$5,290 (1,550)	3,412 (1,000)	-536 (-157)	7.2	-10.2	$93	$7	7.5

* Based on Denver, Colo., climate.
† Based on Allentown, Pa., climate.

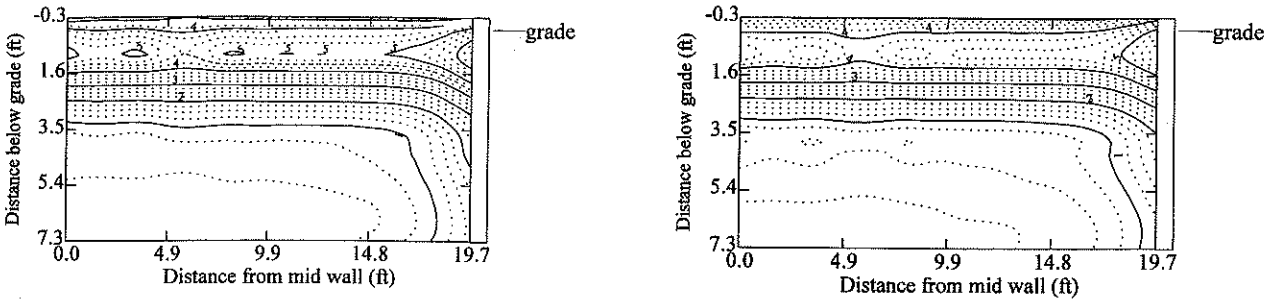

Figure 12a *Unconditioned basement wall heat flux, 21 February, Btu/h·ft^2, Allentown, Pa.: a) uninsulated, b) ceiling insulation.*

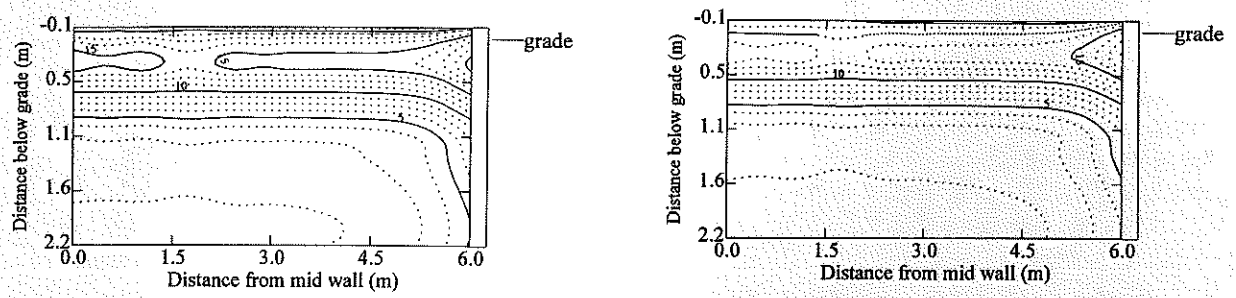

Figure 12b *Unconditioned basement wall heat flux, 21 February, W/m^2, Allentown, Pa.: a) uninsulated, b) ceiling insulation.*

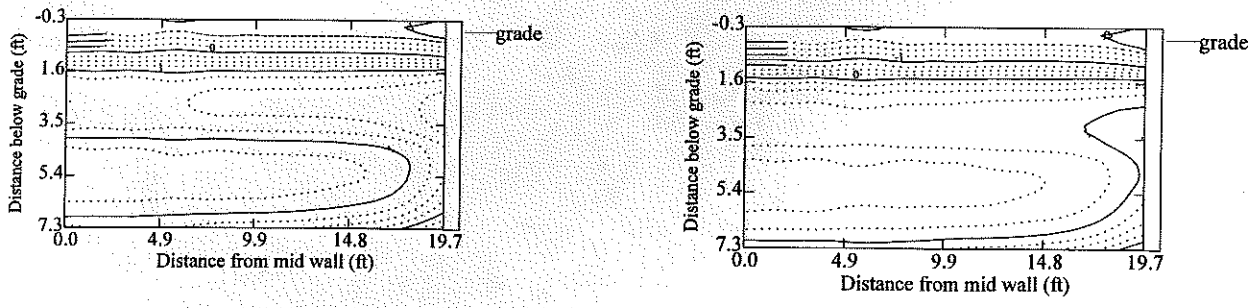

Figure 13a *Unconditioned basement wall heat flux, 21 July, Btu/h·ft^2, Allentown, Pa.: a) uninsulated, b) ceiling insulation.*

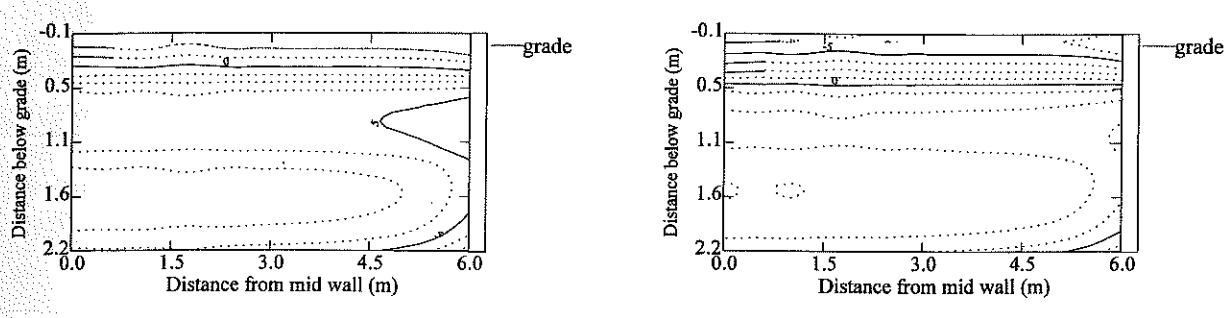

Figure 13b *Unconditioned basement wall heat flux, 21 July, W/m^2, Allentown, Pa.: a) uninsulated, b) ceiling insulation.*

Comparison with Building Foundation Design Handbook

Annual basement heating and cooling loads for Allentown, Pennsylvania, are compared in Table 4 with results for Denver, Colorado, in the *Building Foundation Design Handbook* (Labs et al. 1988). Results are presented for a 1500 ft^2 house with a conditioned basement. Handbook values were scaled to the basement dimensions used in the present study. For Allentown, total basement energy loads were found to represent approximately 25% of whole house loads. This is much less than that previously estimated by other sources (Christian 1991; Labs et al. 1988; Shipp 1983; Wielhouwer 1982) due to the effects of the conditioning dead-band modeled in the present study. Incidental conditioning of the basement by heat gains from mechanical equipment and other internal gains would further diminish this impact.

SUMMARY AND CONCLUSIONS

A three-dimensional numerical model for use in the study of heat transfer in conditioned and unconditioned basements has been described. The model provides considerable flexibility with respect to basement dimensions, foundation materials, insulation placement, and climate. A sophisticated treatment of the boundary conditions enables the program to account for most of the significant parameters that affect earth-coupled heat transfer.

Capabilities of the model have been illustrated through a case study of insulation placement effects for the basement of a typical single-family home located in Allentown, Pennsylvania. Results for the uninsulated, conditioned case are compared against those of an accepted model. Conclusions drawn from the case study are as follows.

- For a heating-dominated climate, the addition of insulation to the foundation wall of a conditioned basement or the ceiling of an unconditioned basement generally results in a reduction in the annual basement-related heating load at the expense of an increase in the cooling load. Because basement heating load is much larger than cooling load, this trade-off is generally beneficial and results in significant energy and energy cost savings.
- Full-height interior wall insulation produced a moderately higher reduction in energy consumption than full-height exterior insulation. Full-height exterior insulation was more effective than partial insulation of the upper half of the foundation wall with twice the full-height R-value.
- Foundation insulation reduces the magnitude of three-dimensional effects. However, corner effects for an uninsulated basement increased heat loss by 6% relative to an estimate based on center-wall values. Consequently, the neglect of corner losses in the uninsulated case will lead to underestimates of savings for use of basement insulation when two-dimensional insulated and uninsulated cases are compared.
- When an attempt is made to model the thermal control of a house in a realistic manner, rather than with the constant indoor temperature assumption applied in many prior studies, the effect is a significant reduction in basement impact on energy consumption. This, combined with the effects of internal loads, may greatly alter the economics of basement insulation. This area is ripe for further research using detailed tools such as the model described in this paper.

REFERENCES

ASHRAE. 1975. *Procedures for determining heating and cooling loads for computerizing energy calculations: Algorithms for building heat transfer subroutines.* Atlanta: American Society of Heating, Refrigerating and Air-Conditioning Engineers, Inc.

ASHRAE. 1997. *1997 ASHRAE Handbook—Fundamentals.* Atlanta: American Society of Heating, Refrigerating and Air-Conditioning Engineers, Inc.

Bahnfleth, W.P. 1989. Three-dimensional modelling of heat transfer from slab floors. Ph.D. dissertation, Department of Mechanical Engineering, University of Illinois, Champaign-Urbana. Also published as USACERL TM E-89/11.

Bligh, T.P., and E.A. Smith. 1983. Thermal conductivity measurements of soils in the field and laboratory using a thermal conductivity probe. EEBS Report No. 25, *Energy Efficient Buildings and Systems.* Cambridge: Massachusetts: Institute of Technology.

Brian, P.L.T. 1961. A finite-difference method of high-order accuracy for the solution of three-dimensional transient heat conduction problems. *A.I.Ch.E. Journal*, 7(3): 367-370.

CABO. 1995. *Model energy code.* Falls Church, Virginia: Council of American Building Officials.

CANMET. 1995. *BASECALC Version 1.0b.* Natural Resources Canada.

Chang, M.J., L.C. Chow, and W.S Chang. 1991. Improved alternating-direction implicit method for solving transient three-dimensional heat diffusion problems. *Numerical Heat Transfer*, vol. 19, Part B, pp. 69-84.

Christian, J.E. 1988. Foundation futures: Energy saving opportunities offered by ASHRAE Standard 90.2P. *ASHRAE Transactions* 94 (2): 979-1002.

Christian, J.E. 1991. Energy efficient residential building foundations—Controlling foundation-related problems can enhance the quality and health of indoor building spaces. *ASHRAE Journal*, November, pp. 36-41.

Cogil, C.A. 1998. Modeling of basement heat transfer and parametric study of basement insulation for low energy housing. M.S. thesis, Department of Architectural Engineering, Pennsylvania State University, University Park.

Douglas, J., Jr. 1962. Alternating direction methods for three space variables. *Numerische Mathematik*, Vol. 4: 41-63.

Eckert, E.R.G., and E. Pfender. 1978. Heat and mass transfer in porous media with phase change. *Proc. of the 6th Annual International Heat Transfer Conference*, pp. 1-12.

Geiger, R. 1961. *The climate near the ground.* Cambridge: Harvard University Press.

Harlan, R.L., and J.F. Nixon. 1978. Ground thermal regime. *Geotechnical engineering for cold regions*, O.B. Andersland and D.M. Anderson, eds., pp. 103-162. New York: McGraw-Hill.

Krarti, M., and S. Choi. 1996. Simplified method for foundation heat loss calculation. *ASHRAE Transactions* 102 (1): 1-13.

Kung, E.C., R.A. Bryson, and D.H. Lenschow. 1964. Study of a continental surface albedo on the basis of flight measurement and structure of the earth's surface cover over North America. *Monthly Weather Review*, 92, Part 12, pp. 543-564.

Kusuda, T., and P.R. Achenbach. 1965. Earth temperature and thermal diffusivity at selected stations in the United States. *ASHRAE Transactions* 71(1): 61-75.

Labs, K., J. Carmody, R. Sterling, L. Shen, Y.J. Huang, and D. Parker. 1988. *Building foundation design handbook.* Oak Ridge National Laboratory, ORNL/Sub/86-72143/1.

Latta, J.K., and G.G. Boileau. 1969. Heat losses from house basements. *Canadian Building*, Vol. 19, No. 10, p. 39.

McQuiston, F.C., and J.D. Parker. 1994. *Heating, ventilating, and air conditioning*, 4th ed. New York: John Wiley & Sons, Inc.

Meixel, G.D., P.H. Shipp, and T.P. Bligh. 1979. The impact of insulation placement on the seasonal heat loss through basement and earth-sheltered walls. *Proc. ASHRAE/DOE.ORNL Conference, Thermal Performance of the Exterior Envelopes of Buildings*, pp. 987-1001. Atlanta: American Society of Heating, Refrigerating and Air-Conditioning Engineers, Inc.

Mitalas, G.P. 1982. Basement heat loss studies at DBR/NRC. National Research Council of Canada, Division of Building Research, NRCC 20416.

Mitalas, G.P. 1987. Calculation of below-grade residential heat loss: Low-rise residential building. *ASHRAE Transactions* 93 (1): 743-783.

NOAA. 1979. Local climatological data (TMY). National Oceanic and Atmospheric Administration, U.S. Dept. of Commerce, Washington, D.C.

Patankar, S.V. 1980. *Numerical heat transfer and fluid flow*, pp. 41-187. New York: Hemisphere.

Pennsylvania Public Utility Commission. 1996a. Electric utility operational report. Pennsylvania Energy Office 1986.

Pennsylvania Public Utility Commission. 1996b. Natural gas utility update. Pennsylvania Energy Office 1986.

Pennsylvania Public Utility Commission. 1997a. Electric utility operational report. Pennsylvania Energy Office 1986.

Pennsylvania Public Utility Commission. 1997b. Natural gas utility update. Pennsylvania Energy Office 1986.

Richmond, W.R., and R.W. Besant. 1985. A study of heat loss through basement floors. *Thermal Performance of the Exterior Envelopes of Buildings II*, pp. 336-350. Atlanta: American Society of Heating, Refrigerating and Air-Conditioning Engineers, Inc.

Sellers, W.D. 1965. *Plant climatology.* Chicago: University of Chicago Press.

Shen, L.S., and J.W. Ramsey. 1988. An investigation of transient, two-dimensional coupled heat and moisture flow in the soil surrounding a basement wall. *International Journal of Heat and Mass Transfer*, Vol. 31, No. 7: 1517-1527.

Shipp, P.H. 1979. The thermal characteristics of large earth-sheltered structures. Ph.D. dissertation, Department of Mechanical Engineering, University of Minnesota.

Shipp, P.H., E. Pfender, and T.P. Bligh. 1981. Thermal characteristics of a large earth-sheltered building (Parts I and II). *Underground Spaces*, Vol. 6: 53-64.

Shipp, P.H. 1983. Basement, crawlspace, and slab-on-grade thermal performance. *Proc. of the ASHRAE/DOE/BTECC Conference, Thermal Performance of the Exterior Envelopes of Buildings II*, pp. 160-179.

Shipp, P.H., and T.B. Broderick. 1983. Comparison of annual heating loads for various basement wall insulation strategies by using transient and steady-state models. *Thermal Insulation, Materials, and Systems for Energy Conservation in the '80s, ASTM STP 789*, F.A. Govan, D.M. Greason, and J.D. McAllister, eds., pp. 455-473. Philadelphia: American Society for Testing and Materials.

Speltz, J.J., and G.D. Meixel. 1981. A computer simulation of the thermal performance of earth covered roofs. *Proc. of the Underground Space Conference and Exposition*, pp. 91-108.

Sterling, R.L., S. Gupta, L.S. Shen, and L.F. Goldberg. 1993. Assessment of soil thermal conductivity for use in building design and analysis. Final report, ASHRAE 701-RP. Underground Space Center, University of Minnesota.

Szydlowski, R.F., and T.H. Kuehn. 1981. Analysis of transient heat loss in earth-sheltered structures. *Underground Spaces*, Vol. 5, pp. 237-246.

U.S. Bureau of the Census. 1995. *Characteristics of new housing: 1995*. Sponsored, all or in part, by the U.S. Department of Housing and Urban Development (HUD). C25/95-A.

Walton, G.N. 1987. Estimating 3-D heat loss from rectangular basements and slabs using 2-D calculations. *ASHRAE Transactions*, 93 (1): 791-797.

Wang, F.S. 1979. Mathematical modeling and computer simulation of insulation systems in below grade applications. *Proc. of the ASHRAE/DOE/BTECC Conference, Thermal Performance of the Exterior Envelopes of Buildings III*, pp. 456-471. Atlanta: ASHRAE.

Werling, E.D. 1994. Design and optimization of energy efficient HVAC systems for modular houses. M.S. thesis, Department of Architectural Engineering, Pennsylvania State University, University Park.

Wielhouwer, A.E. 1982. *Evaluation of basement insulating practices*. University of Waterloo.

Yuill, G.K., and A. Musser. 1997. Evaluation of residential duct-sealing effectiveness. *ASHRAE Transactions* 103 (2): 1-8.